MICROSTRUCTURAL EVOLUTIONS AND MECHANICAL PROPERTIES DURING LONG-TERM AGEING OF TITANIUM ALLOY Ti-17

Nicolas Maury[1,2,3,*], Moukrane Dehmas[2,4], Claude Archambeau-Mirguet[1], Jérôme Delfosse[5], Elisabeth Aeby-Gautier[2,6]

[1]AIRBUS, Toulouse, France

[2]Université de Lorraine, CNRS, IJL, Nancy, France

[3]APSYS-AIRBUS, Vitrolles, France

[4]CIRIMAT, Université de Toulouse, CNRS, Toulouse, France

[5]AIRBUS, Suresnes, France

[6]DAMAS Labex, Université de Lorraine, France

*nicolas.n.maury@airbus.com

Abstract

Microstructural evolutions and resulting mechanical properties have been investigated in the near-β Ti-17 alloy following long- term ageing heat-treatment up to 6000 h at 450 °C. The initial microstructure was bimodal lamellar, consisting of two populations of α grains ($\alpha_{lam\text{-}primary}$ and $\alpha_{secondary}$) in a β phase matrix. Two microstructures were obtained either via controlled heat- treatments from the β phase field - in order to generate significant differences in the grain fraction, size, density and spatial distribution - or sampled from a part submitted to an industrial processing route. High energy XRD reveals that whatever the initial microstructure, the amount of α phase increases significantly after 1000 h long-term ageing. Complementary SEM and image analysis characterizations enable to deduce that this evolution is the consequence of $\alpha_{secondary}$ growth and/or coarsening. Also, TEM observations and EDX analysis show that the Mo and Cr contents of the β phase increase and that α_2 nano-precipitates form within the $\alpha_{lam\text{-}primary}$ grains. Considering the mechanical properties, long-term ageing leads to an increase in the yield and ultimate tensile strength, as well as a decrease in the elongation at failure, at an extent which depends on the ageing time.

Keywords: near-β alloy, ageing, microstructure, crystallography, mechanical properties

1. Introduction

Due to their excellent specific mechanical properties, titanium alloys are widely used for the manufacturing of aeronautical parts. During in-use conditions and as a result of improved engine performances, some of these parts may be submitted to local temperature rises and consequently exhibit changes in the alloy microstructure and mechanical properties.

The present study focuses on the microstructural evolutions during long-term ageing of bimodal lamellar microstructures, consisting of two populations of α grains in a β phase matrix, in the near-β Ti-17 titanium alloy. Such thermal long exposure follows the usual thermal cycle performed on parts after forming steps, which are usually referred to as “ageing” treatments.

Very few studies concerning long-term ageing of titanium alloys can be found in literature, none concerning near-β alloys to the authors’ knowledge. One can mention two studies on near-α alloys: IMI-829 (Ti-5Al-3Sn-3Zr-1Nb-Si) [1] and Ti-1100 (Ti-6Al- 3Sn-4Zr) [2]. After long-term ageing (1000 h at 575 °C and 6000 h at 593 °C, respectively), the yield strength and ultimate tensile strength increase, whereas the elongation a failure decreases. Transmission electron microscopy characterizations evidenced in particular the formation of α_2 phase (Ti_3Al) precipitates, with diameters reported to be between 5 and 20 nm, as well as silicides. Even though the formation of silicides is not expected for Ti-17 alloy, the one of α_2 phase could occur, but its presence before long-term ageing should also be checked.

This latter point is further investigated in the present study. Long-term thermal ageing of 1000 h and 6000 h at 450 °C was performed, either on a specimen sampled from an industrial part submitted to a standard process route, or a specimen submitted to controlled heat-treatments. Microstructural characterizations were performed by electron microscopy, complemented by image analysis and chemical analysis, while the mechanical properties were evaluated by tensile testing.

2. Material and experimental procedure

2.1. Material

The chemical composition of the studied Ti-17 alloy is given in Table 1. The β transus temperature was found to be 887 °C by electrical resistivity measurements. Specimens were sampled from the same radius of the as-received billet, aged and machined into cylindrical specimens for tensile testing.

Table 1: Chemical composition of the Ti-17 alloy

Element	Ti	Al	Mo	Cr	Zr	Sn	Fe	O	Other
Wt. %	Bal.	4.98	4.13	4.11	2.14	2.01	0.03	0.11	< 0.05

2.2. Microstructural and mechanical characterizations

Tensile tests were performed at room temperature (RT) on a Zwick 1484; deformation was measured by an extensometer until failure occurred. Microstructural characterizations were done by a scanning electron microscope (SEM) FEI Quanta 600 field emission gun in backscattered electron mode, operated at 15 kV. Finer scale microstructural characterizations were carried out by transmission electron microscopy (TEM), on thin foils prepared by focused ion beam on a FEI Helios NanoLab 600i DualBeam. Selected area electron diffraction (SAED) patterns and dark field images were then acquired by a JEOL ARM 20F Cold FEG operated at 200 kV, coupled with an EDX analyzer.

Quantification tools were developed to determine in particular the phase volume fractions. These were determined either by image analysis from the SEM micrographs, or by post-mortem high energy X-ray diffraction at the DESY (PETRA III; P07 beamline) or ESRF (ID15A beamline) synchrotron. Details of the image processing routine and the XRD parameters used can be found in [3].

2.3. Heat-treatments and microstructures

Figure 1 shows the two initial microstructures. The "Standard" microstructure (Figure 1(a)) was obtained following high temperature forming, cooling to RT, further annealing at 800 °C and final cooling to RT. During this step, coarse α grains were obtained. Nucleation of α phase occurred at β/β grain boundaries, as well on intragranular sites during the cooling from high temperature. In the first case, growth occurred by wetting along the boundaries to form α layers, whereas in the second case, growth of intragranular α phase occurred with a lamellar morphology of grains. These coarse lamellar grains will be referred to as $\alpha_{lam\text{-}primary}$. Further ageing heat-treatment at 620 °C then enabled the formation of a second population of α grains, of much finer size, to form bimodal lamellar microstructure. These will be referred to as $\alpha_{secondary}$ grains.

The second microstructure was obtained via controlled heat-treatments performed on a self-designed dilatometer. A first annealing in the β-phase field at 920 °C was performed to ensure a fully homogeneous initial state. After cooling to the (α + β) phase field at a rate of 1 °C.s^{-1}, the specimen was isothermally held at 800 °C for 20 h. At this temperature, grain boundary α layers also nucleate and grow along the β/β grain boundaries. Some α layers then grow inside the parent β grain to form colonies of parallel $\alpha_{lam\text{-}primary}$ grains. The resulting microstructure, shown in Figure 1(b), will be referred to as "Colony". Further ageing treatment of 9 h at 620 °C, with a heating rate of 0.05 °C.s^{-1}, was then performed to form the $\alpha_{secondary}$ grains.

These two initial microstructures thus exhibit significant differences in the morphology, size, number density and spatial distribution of $\alpha_{lam\text{-}primary}$ grains. It can also be noticed the highest number density and smallest size of $\alpha_{secondary}$ grains for the "Colony" microstructure.

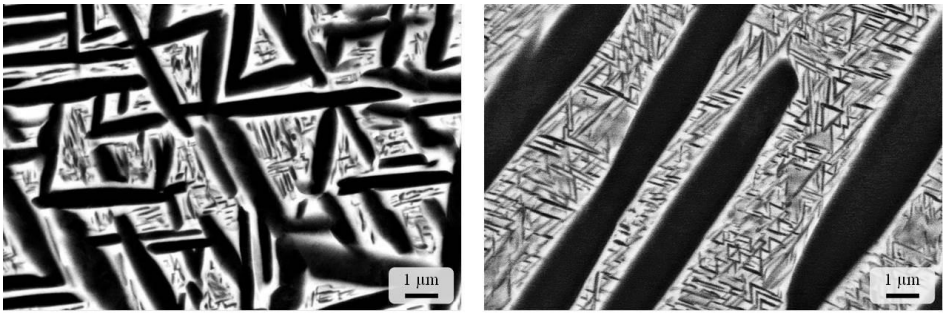

(a) (b)

Figure 1: SEM micrograph of the (a) "Standard" and the (b) "Colony" initial microstructure

Table 2 reports the volume fractions of α grains for the two initial microstructures. The α_{total} fraction, determined by high energy X-ray diffraction, is very similar, about 65%. This takes into account the $\alpha_{lam\text{-}primary}$ and the $\alpha_{secondary}$ grains. However, the $\alpha_{lam\text{-}primary}$ fractions, determined by image analysis, are different: 54% and 33% for the "Standard" and the "Colony" microstructures, respectively. The volume fraction of $\alpha_{secondary}$ grains calculated is thus the lowest for the former (13%) and the highest for the latter (31%).

Table 2: Volume fraction (%) of α_{total}, $\alpha_{lam\text{-}primary}$ and $\alpha_{secondary}$ of the two initial microstructures

Microstructure	Standard	Colony
α_{total}	67 (± 1)	64 (± 1)
$\alpha_{lam\text{-}primary}$	54 (± 2)	33 (± 2)
$\alpha_{secondary}$	13 (± 3)	31 (± 3)

3. Results

3.1. Microstructural characterizations

The "Standard" and "Colony" microstructures were first long-term aged 1000 h at 450 °C. For both, the SEM micrographs (Figure 2) show $\alpha_{secondary}$ grains with a number density and a size that seem to be higher as compared to the unaged microstructures (Figure 1). The tools developed to determine the $\alpha_{lam\text{-}primary}$ and $\alpha_{secondary}$ volume fractions were applied and the results are reported in Table 3. It can be noticed that the $\alpha_{lam\text{-}primary}$ fraction does not evolve (the increase for the "Colony" microstructures is comprised in the uncertainty). The α_{total} volume fraction is about 80%, against about 65% before long-term ageing. Consequently, the $\alpha_{secondary}$ volume fraction after long-term ageing increases by 10 to 15% as compared to the same microstructures unaged. This increase is clearly significant in comparison to the $\alpha_{lam\text{-}primary}$ grains. Also, the final $\alpha_{secondary}$ fraction remains the highest for the "Colony" microstructure.

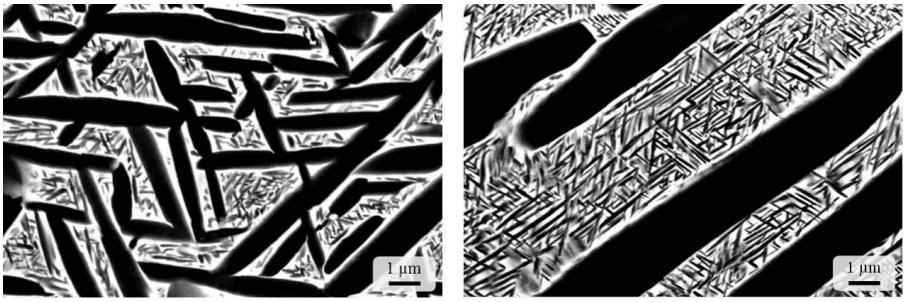

(a) (b)

Figure 2: SEM micrographs of the (a) "Standard" and the (b) "Colony" microstructure after long-term ageing of 1000 h at 450 °C

Table 3: Volume fraction (%) of α_{total}, $\alpha_{lam\text{-}primary}$ and $\alpha_{secondary}$ of the "Standard" and "Colony" microstructure after long-term ageing at 450 °C

Microstructure Long-term ageing time		Colony 1000 h	Standard 1000 h	Standard 6000 h
α_{total}	Unaged	64 (± 1)	67 (± 1)	
	Aged	79 (± 1)	79 (± 1)	80 (± 1)
$\alpha_{lam\text{-}primary}$	Unaged	33 (± 2)	54 (± 2)	
	Aged	37 (± 2)	51 (± 2)	51 (± 2)
$\alpha_{secondary}$	Unaged	31 (± 3)	13 (± 3)	
	Aged	41 (± 3)	28 (± 3)	29 (± 3)

The long-term ageing treatment was extended up to 6000 h for the "Standard" microstructure. The acquired micrograph (Figure 3) does not allow to conclude on significant differences. However, the quantitative analysis (Table 3) shows that the α_{total} volume fraction is similar to the one after 1000 h long-term ageing (increase of 16% as compared to the initial microstructure). Since the $\alpha_{lam\text{-}primary}$ volume fractions are similar at the end of the long-term ageing, the increase in the α_{total} volume fraction is again associated to the one of the $\alpha_{secondary}$ grains.

Figure 3: SEM micrograph of the "Standard" microstructure after long-term ageing of 6000 h at 450 °C

Additional crystallographic characterizations of the α phase were carried out by TEM. SAED patterns were acquired for the "Colony" and "Standard" microstructures aged 1000 h and 6000 h at 450 °C, respectively, focusing on the $\alpha_{lam\text{-}primary}$ grains (Figure 4(a) and (c)). The patterns (Figure 4(b) and (d)) show the characteristic spots of the α phase orientated along the $[0001]_\alpha$ zone axis. It can be noticed for both microstructures additional superlattice spots of less intensity. These can be indexed as spots of the α_2 phase along the $[0001]\alpha_2$ zone axis.

A dark field observation from a superlattice spot of the "Standard" microstructure is shown in Figure 5. This condition allowed to observe nano-scale precipitates with a high number density in the $\alpha_{lam\text{-}primary}$ grain. However, it was not possible to perform such a dark field observation in the "Colony" microstructure.

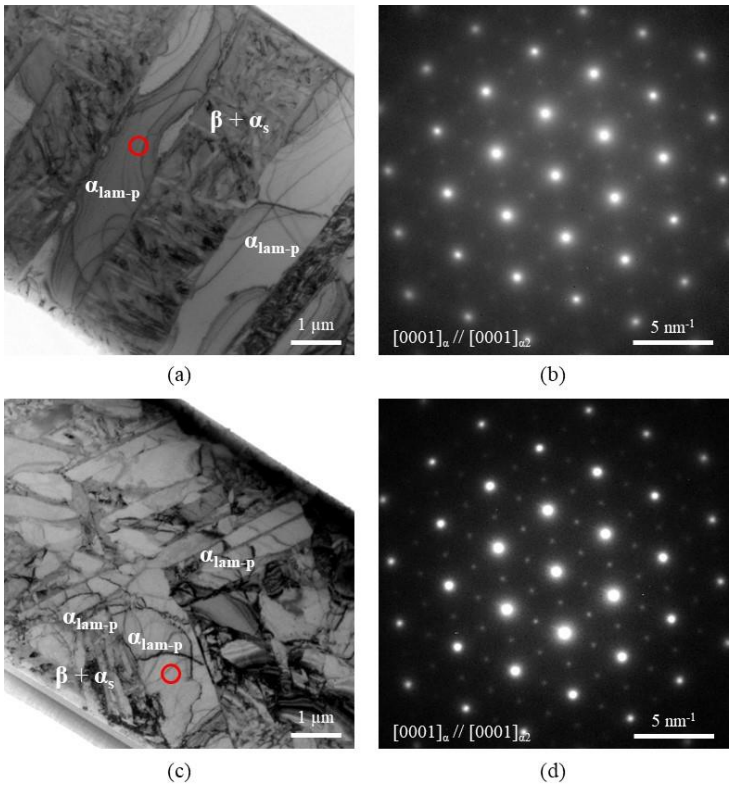

Figure 4: TEM characterization of the "Colony" and "Standard" microstructure after long-term ageing of 1000 h and 6000 h: (a) and (c) bright field with location of the analyzed $\alpha_{lam\text{-}primary}$ grain (red open circle); (b) and (d) corresponding SAED pattern

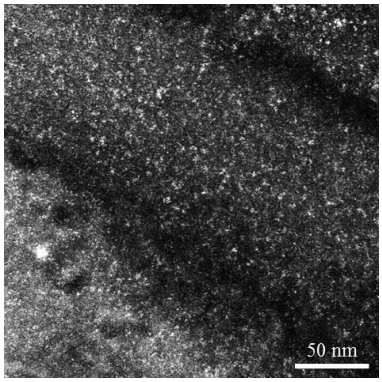

Figure 5: Dark field observation of α_2 nano-precipitates in a $\alpha_{lam\text{-}primary}$ grain of the "Standard" microstructure after long-term ageing of 6000 h

In order to investigate if the formation of the α_2 phase is a microstructural evolution that occurred during long-term ageing, the same crystallographic analysis were carried out on $\alpha_{lam\text{-}primary}$ grains of the unaged "Colony" and "Standard" microstructures (Figure 6(a) and (c)). The SAED pattern of the "Colony" microstructure (Figure 6(b)) shows the characteristic spots of the α and α_2 phases with the same zone axis [0001]; the intensity of the superlattice spots is very low. However, there are no superlattice spots for the "Standard" microstructure (Figure 6(d)). It is worth mentioning that the crystallographic analysis of the $\alpha_{lam\text{-}primary}/\beta$ interface, for all microstructures, did not reveal any other phase.

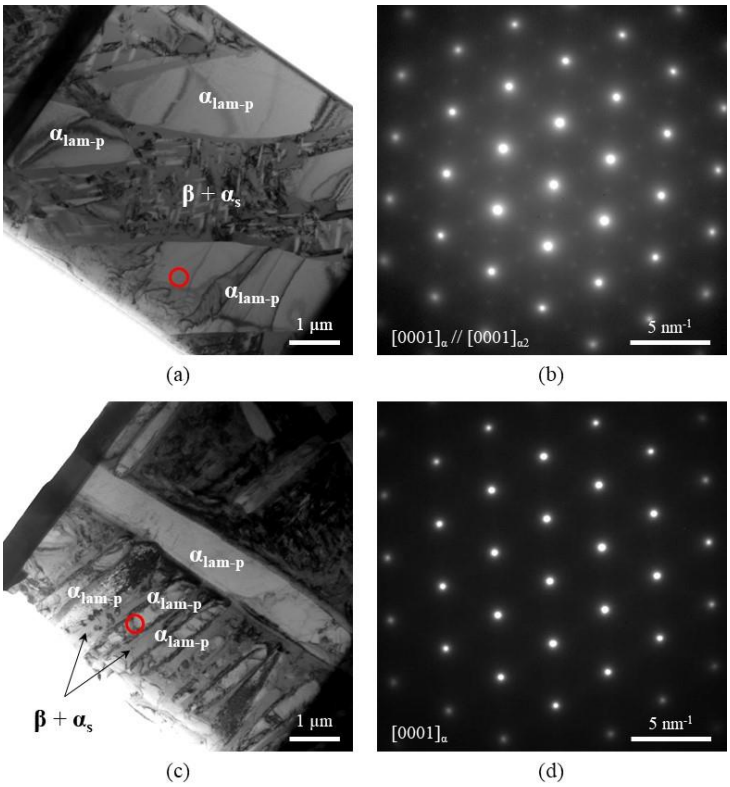

Figure 6: TEM characterization before long-term ageing of the "Colony" and "Standard" microstructure: (a) and (c) bright field with location of the analyzed $\alpha_{lam\text{-}primary}$ grain (red open circle); (b) and (d) corresponding SAED pattern

3.2. Chemical analysis

The chemical composition of the α and β phases of the "Standard" microstructure, before and after long-term ageing of 6000 h at 450 °C, was measured by EDX in TEM. The resulting average values are reported in Table 4. These are compared to the calculations at thermodynamic equilibrium made on the Thermo-Calc software with the TTTI3 database [4] and the chemical composition given in Table 1, before (620 °C) and after (450 °C) long-term ageing.

The chemical composition of the $\alpha_{lam\text{-}primary}$ grains does not evolve significantly and is close to the one predicted, except for the Al contents. However, the chemical composition of the $\alpha_{secondary}$ grains evolves much more significantly. Indeed, the Al content increases by 1.5% whereas the Cr and Mo contents decrease by more than 3%. In the β phase, on the contrary, the Al content decreases by about 1%, so does the Zr and Sn contents by 0.8%. Also, the Cr and Mo contents increase by 2% and 7%, but are more than 4% below the ones predicted.

Table 4: Chemical composition of the $\alpha_{lam\text{-}primary}$ grains, the $\alpha_{secondary}$ grains and the β matrix of the "Standard" microstructure before and after long-term ageing of 6000 h at 450 °C. Comparison with the predictions at the thermodynamic equilibrium

Element (wt. %)			Al	Cr	Mo	Zr	Sn
Experiment	$\alpha_{lam\text{-}primary}$	Unaged	6.7 (± 0.1)	0.4 (± 0.1)	0.4 (± 0.4)	2.0 (± 0.1)	2.4 (± 0.2)
		Aged 6000 h	6.9 (± 0.5)	0.3 (± 0.1)	0.3 (± 0.2)	2.3 (± 0.4)	2.1 (± 0.3)
	$\alpha_{secondary}$	Unaged	4.8 (± 0.5)	3.7 (± 1.9)	4.1 (± 2.0)	2.2 (± 0.3)	2.1 (± 0.3)
		Aged 6000 h	6.3 (± 0.5)	0.5 (± 0.2)	0.5 (± 0.4)	2.3 (± 0.4)	2.2 (± 0.3)
	β	Unaged	2.4 (± 0.1)	10.5 (± 0.1)	11.8 (± 0.5)	1.6 (± 0.2)	1.3 (± 0.1)
		Aged 6000 h	1.3 (± 0.1)	12.8 (± 0.8)	18.7 (± 0.9)	0.7 (± 0.3)	0.6 (± 0.2)
Thermo-Calc calculation	α	620 °C	5.3	0.7	0.5	2.3	2.7
		450 °C	4.6	0.5	0.5	2.6	2.7
	β	620 °C	4.0	13.2	13.8	1.7	0.1
		450 °C	2.4	21.8	22.7	1.1	≈ 0

3.3. Mechanical properties

Normalized tensile properties before and after long-term ageing at 450 °C are reported in Figure 7 for the "Standard" microstructure only. The yield strength (at 0.2% plastic strain) and ultimate tensile strength increase by about 4% and 4.5% respectively after 1000 h exposure, then again by 2% and 1% after 6000 h. However, the elongation at failure decreases by about 50% after 1000 h and after 6000 h exposure. The evolution of the tensile properties is globally more significant during the first 1000 h of long-term ageing.

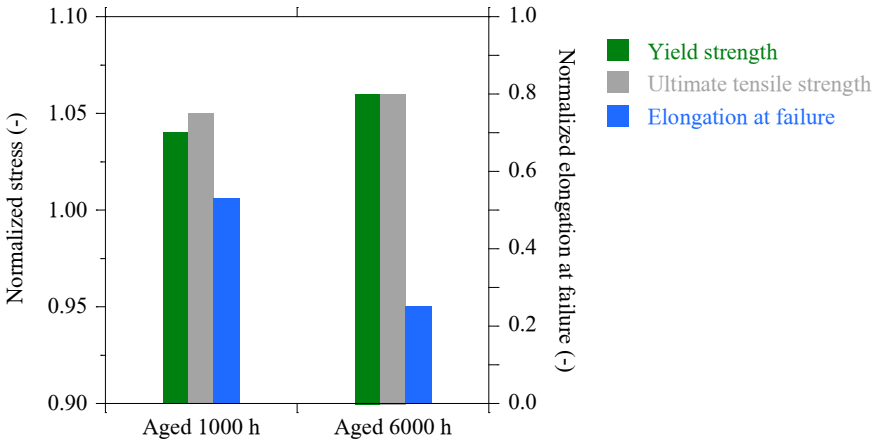

Figure 7: Tensile properties of the "Standard" microstructure after long-term ageing of 1000 h and 6000 h at 450 °C

4. Discussion

4.1. α and β phases

Before long-term ageing, the total α phase volume fraction of the "Standard" and "Colony" microstructures was about 65%. Even though the forming process route is different, the same ageing treatment of 9 h at 620 °C led to a similar amount of α phase. However, it is below the 73% predicted at thermodynamic equilibrium. This difference suggests that the β phase is chemically metastable and could evolve during a further heat-treatment.

Microstructural characterizations after long-term ageing revealed an increase of about 15% of the $\alpha_{secondary}$ volume fraction for each microstructure, to reach a total α volume fraction close to 80% after 1000 h and 6000 h exposure. For comparison, the equilibrium volume fraction predicted at 450 °C is 85%. It is thus close to the one measured experimentally after only 1000 h. The increase in the $\alpha_{secondary}$ fraction could be the consequence of the nucleation and growth of new grains and/or the growth, or even coarsening, of previously formed grains. This statement can hardly be clarified by the SEM observation, since the number density remains high. Moreover, it could be considered that the temperature of 450 °C is relatively low to generate coarsening.

However, focusing on the chemical composition of the $\alpha_{secondary}$ grains of the "Standard" microstructure, a significant decrease in the Mo and Cr contents, as well as an increase in the Al content, is measured after long-term ageing of 6000 h. Also, the chemical composition before ageing is far from the one predicted and it is worth mentioning that a high dispersion was obtained for these first two experimental values. This result cannot be directly explained by an evolution of the chemical composition of these grains. Indeed, it is likely that the analyzed volume contained some β phase, leading to an over-estimation of the Mo and Cr contents and an under-estimation of the Al, and even Zr and Sn contents, as compared to equilibrium calculations.

After long-term ageing, it is supposed that the $\alpha_{secondary}$ grains are coarser. The analyzed volume contains thus very little β phase and the resulting measured chemical composition of α phase is compliant with the calculated data (experimental dispersion is also lower). The decrease in Al content of the β phase, but also the significant increase in Mo and Cr contents in particular, are consistent with the increase of the α phase volume fraction and the evolution of the predicted chemical composition. Nevertheless, thermodynamic equilibrium is not reached.

4.2. α_2 (Ti_3Al) phase

TEM characterizations evidenced the presence of the α_2 phase in the $\alpha_{lam\text{-}primary}$ grains after long-term ageing of both microstructures. The high intensity of the superlattice spots for the "Standard" microstructure after 6000 h exposure suggests a higher fraction and/or number density of α_2 precipitates, as compared to the "Colony" microstructure exposed 1000 h, which supposedly facilitated their observation in dark field.

Small differences in the chemical compositions of the "Standard" and "Colony" initial microstructures could explain the absence of α_2 precipitates in the former one. Thermodynamic calculations show that the temperature of 620 °C is at this phase's boundary, even though its presence was previously reported in this alloy after ageing à 650 °C [5]. Nevertheless, its formation at 450 °C with a fraction higher than at 620 °C, is in agreement with calculations. It can be supposed that the presence of α_2 precipitates is the result of a heterogeneous nucleation in the $\alpha_{lam\text{-}primary}$ grains and that the growth kinetics is slow, mainly due to the temperature and their high number density. It should also be considered the formation of α_2 precipitates in the $\alpha_{secondary}$ grains, but their characterization was unsuccessful due to their small size and high number density.

4.3. Microstructure-mechanical properties relationship

Long-term ageing at 450 °C has led to the same evolution of the tensile properties of the "Standard" and the "Colony" microstructure (not reported). Past studies on near-β alloys (Ti-5553 [6], Ti-17 [5]) and Ti-64 alloy [7] showed, for bimodal microstructures, that dislocations are emitted at the $\alpha_{lam\text{-}primary}/\beta$ interfaces, then glide in the $\alpha_{lam\text{-}primary}$ grains and in the ($\beta + \alpha_{secondary}$) matrix by slip bands. Slips were also observed by in-situ SEM during deformation of the "Standard" microstructure [8]. For the unaged microstructure, they were concentrated at the β/β grain boundary α layers.

As the volume fraction of $\alpha_{secondary}$ grains increases during long-term ageing up to 1000 h, and supposedly their size and number density, the dislocation slips in the β phase are made more difficult by the accumulation of interfaces. Moreover, the α_2 precipitates within the $\alpha_{lam\text{-}primary}$ grains, formed in high number density mainly between 1000 h and 6000 h, act as dislocation accumulation points and affect their gliding, in accordance with previous observations [9]. These two contributions led after long-term ageing to $\alpha_{lam\text{-}primary}$ intragranular failure, on multi-sites and with low plasticity, before intergranular grain boundary α/β deformation [8]. Consequently, the elongation at failure decreases significantly.

5. Conclusion

Bimodal lamellar microstructures, either sampled from an industrial part or designed by controlled heat-treatments to exhibit significant differences in the α grains' microstructural parameters, have been aged at 450 °C up to 6000 h to simulate an in-use service. The results acquired fill a lack of data in the literature for the near-β type alloys.

The tensile strength and elongation at failure increase and decrease respectively, essentially during the first 1000 h, then at a lower extent up to 6000 h. The use of high energy XRD, image analysis and TEM enabled to correlate these mechanical evolutions to microstructural evolutions at a fine scale that are similar whatever the considered initial microstructure. They consist mainly in (i) the increase in the α phase volume fraction ($\alpha_{secondary}$ grains) during the first 1000 h and (ii) the precipitation of α_2 phase in increasing quantity with the long-term ageing duration. These evolutions tend to lead the microstructures to thermodynamic equilibrium (fraction and chemical composition of α, α_2 and β phases), still without reaching it due to low kinetics.

6. Acknowledgements

This work was supported by the French National Research Agency under the DUSTI project (grant number ANR-13-RMNP-0014) and the Labex DAMAS (Design of Alloy Metals for Low-Mass Structures). The authors thank the electronic microscopy center (CC3M) of IJL for helping with the TEM characterizations. The authors also acknowledge the P' Institute for mutual exchanges and all the partners of the project for fruitful discussions.

7. References

[1] A. P. Woodfield, P. J. Postans, M. H. Loretto, and R. E. Smallman, "The effect of long-term high temperature exposure on the structure and properties of the titanium alloy Ti 5331S," *Acta Metallurgica*, vol. 36, no. 3, pp. 507–515, 1988.

[2] A. Madsen, E. Andrieu, and H. Ghonem, "Microstructural changes during aging of a near-α titanium alloy," *Materials Science and Engineering: A*, vol. 171, no. 1, pp. 191–197, 1993.

[3] N. Maury, B. Denand, M. Dehmas, C. Archambeau-Mirguet, J. Delfosse, and E. Aeby-Gautier, "Influence of the ageing conditions and the initial microstructure on the precipitation of α phase in Ti-17 alloy," *Journal of Alloys and Compounds*, vol. 763, pp. 446–458, 2018.

[4] "Thermodynamic databases - Thermo-Calc Software." [Online]. Available: http://www.thermocalc.com/products-services/databases/thermodynamic/. [Accessed: 2019].

[5] N. Escalé, "Étude par microscopie électronique en transmission des microstructures et des micromécanismes de déformation d'alliages de titane béta-métastables," Thèse de doctorat, Toulouse 3, 2012.

[6] T. Duval, "Analyse multi-échelles des relations microstructure/propriétés mécaniques sous sollicitation monotone et cyclique des alliages de titane β-métastable," Thèse de doctorat, Ecole Nationale Supérieure de Mécanique et d'Aérotechnique, 2013.

[7] P. Castany, F. Pettinari-Sturmel, J. Crestou, J. Douin, and A. Coujou, "Experimental study of dislocation mobility in a Ti–6Al– 4V alloy," *Acta Materialia*, vol. 55, no. 18, pp. 6284–6291, 2007.

[8] L. Sasaki, "Influence du vieillissement sur la résistance à la fissuration par fatigue à haute température d'alliages titane pour mâts réacteur," Thèse de doctorat, Ecole nationale supérieure de mécanique et d'aérotechnique, 2018.

[9] N. Escalé, J. Douin, F. Pettinari-Sturmel, C. Daffos, and A. Coujou, "Microstructure and Deformation Micromechanisms of a beta-metastable Titanium alloy Determined by Conventional and in-situ Straining TEM," *Proceedings of the 12th World Conference on Titanium*, 2012.